Fusion Engineering and Design 193 (2023) 113608

Contents lists available at ScienceDirect

Fusion Engineering and Design

journal homepage: www.elsevier.com/locate/fusengdes

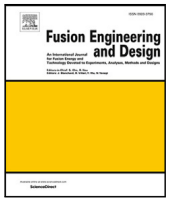

Conceptual design of Fiber Bragg Grating temperature sensors for heat load measurements in COMPASS-U plasma-facing components

J. Caloud [a,b,*], E. Tomesova [a,b], V. Balner [a], O. Bogár [a], Y. Corre [c], R. Dejarnac [a], M. Dimitrova [a], J. Gerardin [a], M. Hron [a], R. Pánek [a], K. Patocka [a], M. Peterka [a,d], P. Vondracek [a], V. Weinzettl [a]

[a] Institute of Plasma Physics of the CAS, Prague, Czech Republic
[b] FNSPE, Czech Technical University in Prague, Prague, Czech Republic
[c] CEA Cadarache, IRFM, F-13108 St Paul lez Durance, France
[d] Faculty of Mathematics and Physics, Charles University in Prague, Prague, Czech Republic

ARTICLE INFO

Keywords:
Heat loads
Plasma-facing components
Diagnostics
Fiber Bragg Gratings
Temperature measurements

ABSTRACT

Information about the temperature of plasma-facing components is important for a reliable tokamak operation. A temperature monitoring system using Fiber Bragg Grating (FBG) sensors is foreseen for the new tokamak COMPASS Upgrade, which is currently starting its construction. This diagnostic can be a valuable complement to IR thermography, thermocouples, and Langmuir probe divertor diagnostics. The system will be optimized to estimate the steady-state and transient heat loads, such as runaway electrons, on the divertor and limiters. In this contribution, current progress in the design of the FBG sensors for the COMPASS-U initial open divertor and guard limiters is presented. The heat flux on the plasma-facing components is modeled for diverted and first phase circular plasma scenarios by the PFCFlux code. The subsequent heating and the mechanical strain in the components dedicated for the placement of the sensors is simulated by the finite element analysis software ANSYS. Using these results, the optimal placement and configuration of the sensors are determined with respect to the anticipated maximum temperature and gradients.

1. Introduction

The COMPASS Upgrade [1,2] tokamak is currently starting its construction. It will be a new high magnetic field (B_T = 5 T) and high density ($n_e \sim 10^{20}$ m^{-3}) tokamak installed at the Institute of Plasma Physics of the CAS. Its plasma-facing components (PFC) will be fully metallic, the components most exposed to plasma will be manufactured from the bulk tungsten, while the remaining PFC will be made from tungsten-coated Inconel. The vacuum vessel is planned to be capable of operation at high temperatures (up to 500 °C), which has to be considered in the diagnostics design [3].

The heat loads on the initial open divertor strike points during the high-performance attached H-mode discharges will reach > 10 MW/m^2, according to the PFCFlux simulations [4] of discharge scenarios modeled by METIS [5]. This H-mode scenario will employ 4 MW of NBI heating and 2 MW of ECRH heating with the maximum duration of the flat-top up to 3 s. Due to that, it is necessary to monitor PFC temperature not only for machine protection but also for the characterization of the plasma heat flux in this region. For this purpose, there will be different types of temperature sensors embedded in the COMPASS-U PFC. Mineral Insulated Cable thermocouples are planned mainly for machine monitoring, whereas the PFC heat loads will be estimated from the temperature measurements by Fiber Bragg Grating temperature sensors.

The Fiber Bragg Grating (FBG) sensors are suitable for measurements at the tokamak extreme environment thanks to their high maximum operating temperature and immunity to electromagnetic interference. For COMPASS-U, a full poloidal coverage of the PFC temperature measurements is planned. For the first phase of operation, FBG sensors in inner and outer guard limiters and initial open divertor are prepared. In later phases of operation, closed tungsten divertor will be added. The FBG calorimetry system is foreseen for this component as well. This article describes the progress in the conceptual design of the Fiber Bragg Grating temperature sensor system for the first phase of the COMPASS-U operation. The FBG sensors are introduced in Section 2 and the following sections describe the preliminary conceptual design of each considered component and ANSYS simulations, which were used for the design.

* Corresponding author at: Institute of Plasma Physics of the CAS, Prague, Czech Republic.
E-mail address: caloud@ipp.cas.cz (J. Caloud).

https://doi.org/10.1016/j.fusengdes.2023.113608
Received 31 October 2022; Received in revised form 29 January 2023; Accepted 24 February 2023
Available online 10 April 2023

2. Fiber Bragg Grating temperature sensors

The working principle of the Fiber Bragg Grating sensors is based on the Bragg interference of the light on the gratings in the optical fiber. The gratings are regions of periodically changing index of refraction inscribed in the fiber. The wavelength of the light reflected on the gratings λ_B is defined by the grating period Λ and effective refractive index of the fiber core n_{eff}.

$$\lambda_B = 2 n_{eff} \Lambda \tag{1}$$

The Bragg wavelength of the grating can vary due to changes in the refractive index of the fiber or the periodicity of the gratings. This can be caused by a change of the fiber temperature or by strain applied on the fiber [6].

$$\Delta\lambda_B = 2\left(\Lambda\frac{\partial n}{\partial l} + n_{eff}\frac{\partial \Lambda}{\partial l}\right)\Delta l + 2\left(\Lambda\frac{\partial n}{\partial T} + n_{eff}\frac{\partial \Lambda}{\partial T}\right)\Delta T \tag{2}$$

In Eq. (2), the first term gives the change of λ_B due to the applied strain, while the second term shows the effect of temperature change of the fiber. Thermal expansion of the fiber changes the spacing of the grating and the refractive index changes due to thermo-optic effects. The wavelength shift due to temperature change can be expressed as

$$\Delta\lambda_B = (\alpha + \zeta)\lambda_B \Delta T \tag{3}$$

where α is the thermal expansion coefficient and ζ is the thermo-optic coefficient of the fiber. From Eq. (3), it can be seen, that the Bragg wavelength shift depends linearly on the temperature change of the fiber. The temperature of the sensing point (defined by the grating) can therefore be determined from the wavelength shift of λ_B if zero strain on the fiber is ensured.

The sensing points can be multiplexed on one fiber, allowing for a large number of sensors with one fiber in the tokamak vessel. In this case, each sensing point is inscribed with a different grating period and therefore the Bragg wavelength. The number of gratings on one fiber is limited by the wavelength range of the laser and interrogator used for the measurements. The wavelength spacing of the gratings is limited by the temperature gradient along the fiber, so the peaks in the reflected spectrum do not overlap.

Thanks to the optical principle of measurement, FBG sensors are immune to electromagnetic interference. The operating range of temperatures is limited by the erasure of the gratings. Typically, FBG sensors can withstand temperatures up to 600 °C after thermal annealing [7]. Thanks to innovative methods of grating inscription, such as regenerated or femtosecond FBG, this limit can be increased up to 1200 °C.

Such high-temperature operation of the FBG sensors was demonstrated at the WEST tokamak, where the fibers were installed in two generations of divertor [8,9]. It was shown, that the temperature profiles along the fiber can be used to determine the heat load profiles on the divertor using the thermal inversion [10].

3. COMPASS Upgrade plasma-facing components

The plasma-facing components of COMPASS Upgrade are designed to withstand heat fluxes in order of tens of MW/m^2 on the inner limiters and divertor. The most exposed components — inner and outer guard limiters will be installed for the first plasma operation and will be manufactured from bulk tungsten. There will be a total of 8 inner guard limiters and 2 outer guard limiters, one of each type is planned to be equipped with an FBG temperature measuring system. The inner guard limiters are located on the central column and the outer guard limiters are rib-shaped limiters located on the low field side of the vessel. The other limiters (16 inner and 8 outer) will be recessed radially a few millimeters outwards from plasma, so that they will be less thermally loaded. Therefore, these limiters will be manufactured from Inconel. Inconel will be used for the initial open divertor (IOD) as well, which will be installed as an upper divertor for the first phase of COMPASS-U operation. The bulk tungsten lower divertor is planned for later phases of operation. The overview of the COMPASS-U PFC is in Fig. 1, where the parts equipped by FBG system for the first phase of operation are highlighted in orange. The main parameters of simulated scenarios are listed in Table 1. For the design of FBG system in the inner guard limiter, a high performance limited discharge scenario 1600 was used, whereas for the design of the inconel open divertor, a diverted H-mode scenario 3200 with lower parameters was used.

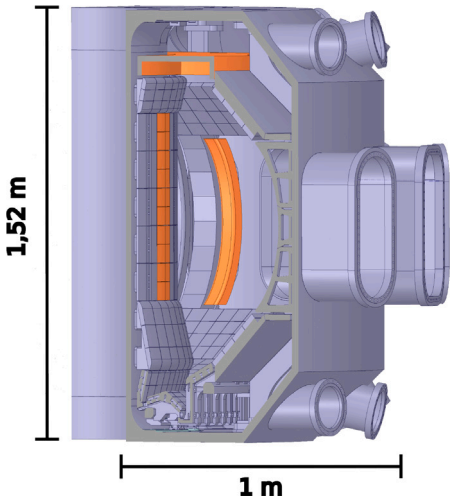

Fig. 1. Cut through the CAD model of COMPASS-U plasma-facing components and vacuum vessel with inner and outer guard limiters and initial open divertor highlighted.

Table 1
Main parameters of the simulated COMPASS-U operation scenarios.

Parameter	Scenario 1600	Scenario 3200
B_T [T]	5	2.5
I_p [MA]	1	0.8
$t_{flat-top}$ [s]	2.6	3.2
P_{NBI} [MW]	3	2
P_{ECRH} [MW]	1	–
P_{SOL} [MW]	4.3	2.0
$\lambda_{q,near}$ [mm]	1.9	–
$\lambda_{q,main}$ [mm]	9.2	1.35

3.1. Inner Guard Limiter

The Inner Guard Limiter (IGL) [11] will be one of the PFC installed from the first phase of the COMPASS-U operation. The component will be machined from bulk tungsten to withstand the heat loads during limited discharges and plasma current ramp-up and ramp-down phases. During the high-performance inner limited discharge — scenario 1600 (parameters are listed in Table 1) the peak heat load on the poloidal chamfers of tiles directly under and above the midplane is expected to be up to 85 MW/m^2, which was calculated by optical approximation with the 3D field line tracing code PFCFlux [4]. The simulated heat flux on the IGL is in Fig. 2(a). In the same figure on the right, the surface temperature of the tile at the time t = 700 ms is shown when the temperature threshold of 2000 °C (engineering limit) was reached and the source of the heat flux was turned off.

The heat flux from PFCFlux simulation is used as input for ANSYS [12] transient thermal analysis of given PFC tiles. Based on these simulations, the conceptual location of the fiber in the IGL was chosen, which can be found in Fig. 3 in the horizontal cut of the component. Safe depth for FBG operation inside the tile is defined by the maximum temperature at the given depth. We have fixed an operational limit for the FBG at 1000 °C at any point of the probe. In the IGL case,

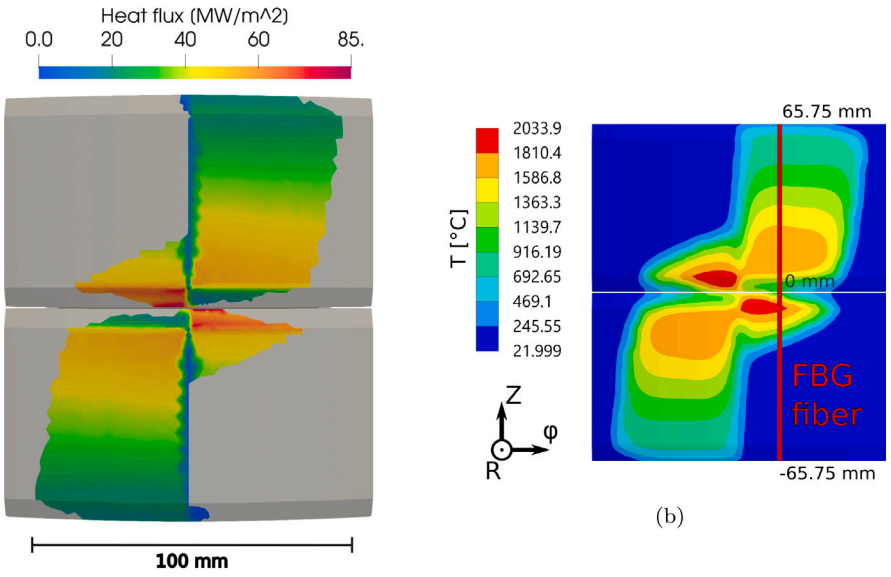

Fig. 2. Incident heat flux on the Inner Guard Limiter tiles simulated by PFCFlux for scenario 1600 (a) and the surface temperature at 700 ms modeled in ANSYS with marked position of the fiber (b).

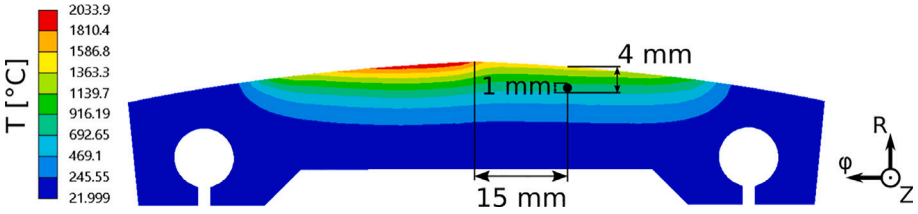

Fig. 3. Horizontal cut of the IGL at the time $t = 700$ ms with marked position of the fiber (black dot).

this corresponds to a depth of 3.5 mm below the tile surface. The FBG fibers are typically enclosed in a capillary with 1 mm diameter. The safe position for the center of the fiber is therefore 4 mm under the part surface. The analysis of stresses on the fiber due to thermal expansion of the components will be performed after the finalization of the PFC design.

The minimum spacing of the sensing points along the fiber is defined by the width of the gratings, which is typically $1 - 5$ mm. For this conceptual design, the width of the grating was considered 3 mm and the spacing 10 mm. The spacing of the peaks from each grating in the wavelength space (λ-spacing) is limited by the thermal gradient between the adjacent gratings, so the peaks in the spectrum do not overlap. The plot of the temperature and its gradient along the fiber at the time, when the fiber reaches its maximum temperature ($t = 744$ ms) for the 4 mm depth is in Fig. 4. The typical sensitivity of regenerated FBG is 16.3 pm/°C. The maximum temperature gradient on the inner edge of the component is 60 °C/mm. For a conservative estimate of the λ spacing a constant temperature gradient of 60 °C/mm on the 10 mm spacing between two gratings was assumed. Based on these parameters, the maximum λ-spacing of the gratings is 9.8 nm. The λ-range of commercially available FBG interrogators is 30−160 nm. It will be therefore possible to fit up to 16 gratings equidistantly spaced on one fiber, which is enough to cover the IGL tiles with 10 mm spacing. In the case of the IGL tile, the proposed configuration uses 12 gratings with 10 mm spacing to cover the whole component in the vertical direction. The temperature of the gratings along the fiber is in Fig. 4.

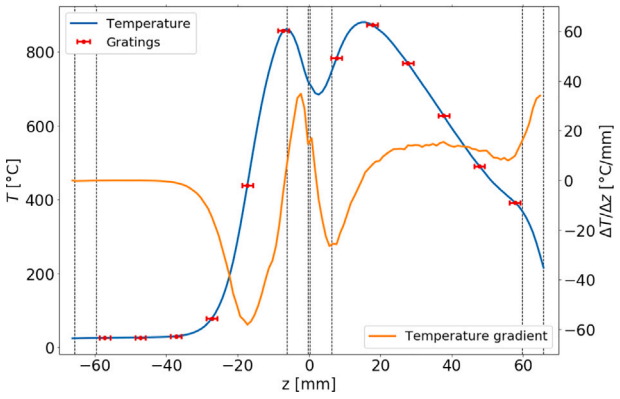

Fig. 4. Temperature profile and its gradient along the fiber at $t = 744$ ms in the IGL with marked position of the gratings (red lines).

3.2. Initial open divertor

The initial open divertor (IOD) is planned for the first phase of COMPASS-U operation. It will be manufactured from Inconel and installed as the upper divertor. The FBG thermal diagnostic is proposed to secure the component protection against heat loads and estimation of the perpendicular heat flux on the divertor. The predicted heat flux is modeled by PFCFlux for a diverted H-mode scenario 3200 (parameters are listed in Table 1). The heat flux profile has been used as an input for the ANSYS transient thermal analysis (Fig. 5). The considered

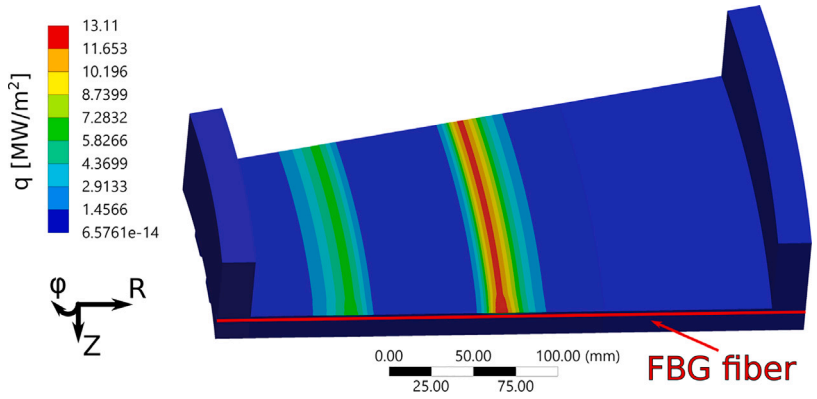

Fig. 5. Surface heat flux on the IOD (q_{max} = 13 MW/m^2) calculated by PFCFlux with marked position of the FBG fiber.

Table 2
Maximum temperature obtained by FBG and temperature gradient for different depths of the fiber in the IOD.

Depth [mm]	$T_{FBG,max}$ [°C]	dT/dx [°C/mm]	Δz [mm]
2	180	15	0.138
3	120	8	0.095
4	95	6	0.077

engineering temperature limit of Inconel is 900°C, which is lower than the temperature limit of the FBG fibers. In the studied scenario, the temperature limit was achieved after 180 ms. The depth of the fiber inside the component will therefore be determined mainly by material deformation.

The fiber in the IOD will be placed in a groove machined in the radial direction on the vertical edge of the component. The position of the fiber is visible in Fig. 6(a) of the vertical divertor cut and it corresponds to the location of the outer strike point. The ANSYS thermal simulations were performed for three configurations of the fiber depths 2, 3, and 4 mm below the divertor surface. The maximum temperature and its gradient for the mentioned configurations are listed in Table 2. For these configurations, a transient structural analysis was performed as well. The maximum deformation due to the temperature gradients for each configuration is listed in Table 2.

The temperature profile and the temperature gradient along the length of the fiber in the 3 mm depth are shown in Fig. 7. Due to the relatively low maximum temperature gradient of 8 °C/mm, the λ-spacing of the gratings can be only 1.3 nm assuming 10 mm spacing of gratings. Therefore, the number of gratings will not be limited by the temperature gradient. The configuration in Fig. 7 shows 34 gratings with 3 mm length and 10 mm spacing. The deformation of the Inconel tile above the groove with the fiber for the configuration with the fiber in 3 mm depth is shown in Fig. 6(b). In this configuration, the maximum deformation is < 0.1 mm. The maximum surface temperature of the divertor is reached after 180 ms. The deformation reaches maximum at the same time, however the maximum temperature detected by the fiber in the groove is reached at the time t = 1405 ms (which is shown in Fig. 6(a)) due to relatively low thermal conductivity of Inconel. In the final design, the groove will be filled with a glue, which will reduce the deformation. Moreover, the edges of the divertor could be chamfered, to prevent overheating of the deformed or misaligned edges. The simulations with the glue in place and finished IOD design will be performed in near future. The precise position and configuration of the FBG diagnostic will be determined based on these calculations.

3.3. Outer guard limiter

The outer guard limiter (OGL) is planned to be installed for the first plasma as well as the IGL. It will be a bulk tungsten poloidal rib limiter on the low field side protruding radially inward in comparison with other outer limiters to protect the stabilizing plate bridge [2]. According to PFCFlux simulations, the OGL is too far from the plasma to receive significant heat fluxes. This component is therefore designed mainly for the protection of the first wall during transient events, such as Runaway Electrons (RE) and disruptions.

The runaway electrons generated during a discharge under certain conditions can carry a significant part of the plasma current and when they strike the wall, they can deposit heat loads of several hundreds of MW/m^2. Due to the outward drift of RE, the most affected PFC are the outer limiters or divertor due to vertical displacement events. The FBG temperature monitoring system is proposed for the OGL to study the heat load levels and deposition profiles (wetted area) on the component in the case of RE impact. Due to very short time of the RE impact on the PFC, the main aim of the diagnostic in the OGL will be the estimation of the total (time integrated) energy deposited in the component and its spatial distribution, as it was done by the calorimetry probe at COMPASS [13].

Runaway electrons with energy more than 10 MeV can deposit their energy in significant depths inside solid materials. For example, the range of 10 MeV RE incident on tungsten with angle 10° is 3.2 mm [14].

The energy deposition by RE on the tungsten OGL was simulated by Monte Carlo particle code FLUKA [15]. FLUKA can simulate the transport and interactions of high energy electrons (E > 1 keV) with solid materials and create profiles of the deposited energy density in 3D CAD geometry of the components. In this work, the impact of 10 MeV electrons on the tungsten limiter was simulated with the local magnetic field from circular discharge scenario 1600 (parameters are listed in Table 1). The map of the deposited energy density is in Fig. 8. This profile of the deposited energy was then used as an input (volumetric heat generation) for the ANSYS thermal analysis to determine the surface melting limits for the incident heat flux. Heat loads in the range from 10 to 50 MJ/m^2 during 10 to 100 ms (time of RE deposition) and the incident spot size of 3.1 cm^2 were simulated. The surface melting heat loads were found to be > 300 MW/m^2 for 100 ms and > 1 GW/m^2 for 10 ms. For the final design of the FBG sensors in the outer guard limiter, particle tracing simulations of the RE beam are planned to characterize the spatial and energy distribution of impacting electrons on the OGL.

4. Summary and outlook

The conceptual design of Fiber Bragg Grating temperature sensors for COMPASS Upgrade is presented in this contribution. The analysis was performed for three plasma-facing components, which are considered for the installation of FBG sensors from the first phase of COMPASS-U operation. The temperatures of the inner guard limiter and initial open divertor were simulated using ANSYS with the inputs from PFCFlux models of plasma heat loads on the PFC. The outer guard limiter is considered for the studies of runaway electron impact, as

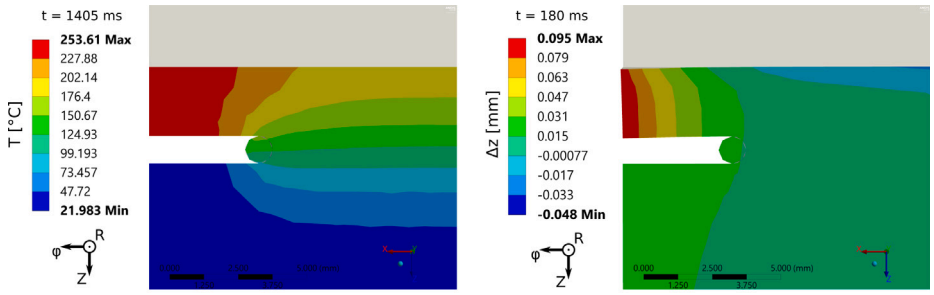

Fig. 6. Temperature profile at time t = 1405 ms (a) and thermal deformation at time t = 180 ms (b) in the IOD vertical cut depth at the outer strike point with the FBG at the 3 mm.

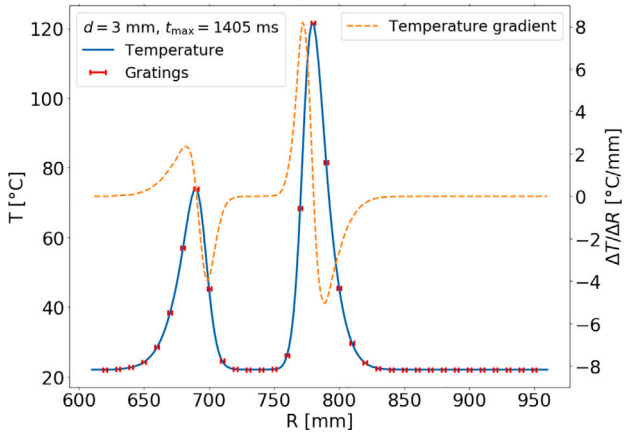

Fig. 7. Temperature profile and its gradient along the fiber (3 mm below surface) in the IOD with marked position of the gratings.

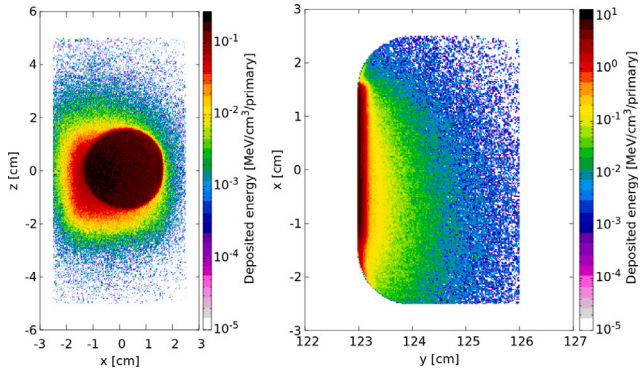

Fig. 8. Map of the energy density deposited by 10 MeV monoenergetic beam of runaway electrons with 10° incidence angle in the outer guard limiter simulated in FLUKA.

the thermal plasma heat loads on the OGL in the studied scenarios are predicted to be negligible.

In the near future, it is planned to find a solution for the fiber attachment in the components (including the thermal glue) and prepare the corresponding modification of the tiles using the ANSYS structural simulations. The effect of the thermal response time on the resolution of the diagnostic will be simulated. The thermal inversion algorithm is planned to be implemented before the final design of the diagnostic and tested for the simulated FBG temperatures to obtain the heat flux reconstruction for different configurations of the FBG sensors for stationary heat fluxes. Moreover, the runaway electron impact will be modeled with broader range of energy (not only he average one) to prepare the final design of the fibers in the OGL. For RE transient heat loads simulations analyzing the total deposited energy and spatial resolution of the diagnostic are planned. Tests at a high heat flux facility are planned after the FBG design phase will be completed.

Declaration of competing interest

The authors declare that they have no known competing financial interests or personal relationships that could have appeared to influence the work reported in this paper.

Data availability

Data will be made available on request.

Acknowledgments

This work has been carried out within the framework of the EUROfusion Consortium, funded by the European Union via the Euratom Research and Training Programme (Grant Agreement No 101052200 — EUROfusion). Views and opinions expressed are however those of the author(s) only and do not necessarily reflect those of the European Union or the European Commission. Neither the European Union nor the European Commission can be held responsible for them.

References

[1] R. Panek, T. Markovic, P. Cahyna, R. Dejarnac, J. Havlicek, J. Horacek, M. Hron, M. Imrisek, P. Junek, M. Komm, et al., Conceptual design of the COMPASS upgrade tokamak, Fusion Eng. Des. 123 (2017) 11–16.

[2] P. Vondracek, R. Pánek, M. Hron, J. Havlicek, V. Weinzettl, T. Todd, D. Tskhakaya, G. Cunningham, P. Hacek, J. Hromádka, et al., Preliminary design of the COMPASS upgrade tokamak, Fusion Eng. Des. 169 (2021) 112490.

[3] V. Weinzettl, J. Adamek, P. Bilkova, J. Havlicek, R. Panek, M. Hron, O. Bogar, P. Bohm, A. Casolari, J. Cavalier, et al., Constraints on conceptual design of diagnostics for the high magnetic field COMPASS-U tokamak with hot walls, Fusion Eng. Des. 146 (2019) 1703–1707.

[4] M. Firdaouss, V. Riccardo, V. Martin, G. Arnoux, C. Reux, et al., Jet-efda Contributors, Modelling of power deposition on the JET ITER like wall using the code PFCFLux, J. Nucl. Mater. 438 (2013) S536–S539.

[5] J. Artaud, V. Basiuk, F. Imbeaux, M. Schneider, J. Garcia, G. Giruzzi, P. Huynh, T. Aniel, F. Albajar, J. Ané, et al., The CRONOS suite of codes for integrated tokamak modelling, Nucl. Fusion 50 (4) (2010) 043001.

[6] A. Othonos, Fiber bragg gratings, Rev. Sci. Instrum. 68 (12) (1997) 4309–4341.

[7] M. Cavillon, M. Lancry, B. Poumellec, Y. Wang, J. Canning, K. Cook, T. Hawkins, P. Dragic, J. Ballato, Overview of high temperature fibre bragg gratings and potential improvement using highly doped aluminosilicate glass optical fibres, J. Phys.: Photon. 1 (4) (2019) 042001.

[8] Y. Corre, G. Laffont, C. Pocheau, R. Cotillard, J. Gaspar, N. Roussel, M. Firdaouss, J.-L. Gardarein, D. Guilhem, M. Missirlian, Integration of fiber bragg grating temperature sensors in plasma facing components of the WEST tokamak, Rev. Sci. Instrum. 89 (6) (2018) 063508.

[9] N. Chanet, Y. Corre, R. Cotillard, J. Gaspar, G. Laffont, C. Pocheau, G. Caulier, C. Dechelle, B. De Gentile, C. Destouches, et al., Design and integration of femtosecond fiber bragg gratings temperature probes inside actively cooled ITER-like plasma-facing components, Fusion Eng. Des. 166 (2021) 112376.

[10] J. Gaspar, Y. Corre, M. Firdaouss, J. Gardarein, J. Gerardin, J. Gunn, M. Houry, G. Laffont, T. Loarer, M. Missirlian, et al., First heat flux estimation in the lower divertor of WEST with embedded thermal measurements, Fusion Eng. Des. 146 (2019) 757–760.

[11] J. Gerardin, et al., Front face shaping of the inner wall tiles in the COMPASS Upgrade tokamak, Poster #62 at 32nd Symposium on Fusion Technology (SOFT2022), September 18 – 23, 2022, Dubrovnik, Croatia. Also Fusion Eng. Des. 2022, submitted for publication.

[12] ANSYS® Academic Research Mechanical, Release 21.1.

[13] J. Caloud, et al., Calorimetry probe measurements of the runaway electron impact energy on plasma facing components at COMPASS tokamak, in: P2b.118 at 48th EPS Conference on Plasma Physics, June 27 – July 1, 2022, Amsterdam, The Netherlands, http://ocs.ciemat.es/EPS2022PAP/pdf/P2b.118.pdf, [online].

[14] M.J. Berger, et al., Estar, pstar, and astar: computer programs for calculating stopping-power and range tables for electrons, protons, and helium ions (version 1.21), http://physics.nist.gov/Star, [online] (1999, Accessed October 3, 2022).

[15] G. Battistoni, T. Boehlen, F. Cerutti, P.W. Chin, L.S. Esposito, A. Fassò, A. Ferrari, A. Lechner, A. Empl, A. Mairani, et al., Overview of the FLUKA code, Ann. Nucl. Energy 82 (2015) 10–18.